

# Experimental Analysis of FSW Process Forces

Tadeusz Balawender\*, Piotr Myśliwiec

*The Faculty of Mechanical Engineering and Aeronautics Rzeszow University of Technology,  
Powstańców Warszawy 8 Str., 35-959 Rzeszow, Poland*

## Abstract

*This paper presents the results of research work on linear friction stir welding (FSW) of magnesium AZ31 and aluminum 2024 alloys. During the FSW process, forces exerted by a tool on joined materials were measured. The measurements of forces were taken in three directions, vertical (Z axis) and horizontal (X and Y axes) directions, using high-sensitive piezoelectric dynamometer. The force analysis was done for three stages of welding process: plunging, dwelling, and welding. Conclusions regarding the force reaction of materials to be welded were formulated. It was found that the first two stages of the process, plunging and dwelling, are very important for the correct welding. In the plunging stage, a tool exerts the greatest forces and unit pressures (at the Z direction) on joined materials; during the dwelling stage, thermal conditions of the process are established. The welding stage was divided into two substages: the initial unstable and the subsequent long-term stabilized one.*

## Keywords

*friction stir welding, aluminum alloy 2024, magnesium alloy AZ31, force measurement, welding force*

## 1. Introduction

Friction stir welding (FSW) process is one of the most important solid-state joining techniques, which has unlimited applications in many areas of industries, including automotive and aviation. Due to weight reduction (no additional connector), tightness, and high strength of the joint, FSW welding is particularly an attractive joining technique in the aerospace industry for high-performance structural applications. This technology enables joining highly alloyed aluminum series of 2xxx and 7xxx, which make problems for conventional welding because of a poor solidification microstructure and porosity in the fusion zone [1].

The idea of the FSW process is quite simple: a rotating tool (with a specially designed pin and shoulder) is plunged into joined materials and forced to move along a joint line. In the first stage of the process, as a result of rotational movement of the tool and friction of its working surfaces with surfaces of joined materials, heat is released, which increases the temperature of joined materials. The growth of temperature causes the drop of materials' flow stress that results in plunging of the tool into joined materials. The rotating tool, immersed in the joined materials, causes their vortex movement and mutual mixing in a solid state. Additional heat is also generated as a result of plastic deformation. So, there are two primary functions of the tool: heating and forcing a

material stirring to produce the joint. As it was shown in the work of Heurtier et al. [2], heat comes from three sources: from friction of a tool pin, from friction of a tool shoulder on a joined materials surface, and from plastic strain. The contribution of plastic deformation in heating materials was estimated by Lorrain et al.[3] from numerical simulations as the ratio of a plastic to frictional dissipation is about 0.29. The tool feed motion is along the joint line to form a tough weld and this quality results mainly from the action of the tool shoulder, which additionally compacts materials below it and prevents the weld from oxidizing. The characteristic feature is implementation of the process at temperature lower than the melting temperature of joined materials. The process temperature can be calculated based on the equation shown in the literature [1, 4], taking into account the process parameters for a given tool geometry and a depth of penetration. But in most publications it is simply assumed that the FSW process temperature rises to approximately 0.8 melting point as it was implemented by Roy et al. [5] and Malarvizhi and Balasubramanian [6].

The course of the process and the quality of FSW joint are dependent on many factors. The most important of them are geometry of forming tool, its rotational and linear velocities, thrust force and deviation from perpendicular direction to joined surfaces, and its penetration into joined materials. During

\* Corresponding author: Tadeusz Balawender  
E-mail: tbalaw@prz.edu.pl

the FSW process, complex material movement and large plastic deformations occur. The geometry of the tool and technological parameters of the welding process determine a degree of “mixing” of materials, process temperature, structure and strength of the weld, as it was proved experimentally by Balawender and Micał [7] and Myśliwiec et al. [8]. The forces exerted by the tool during the FSW process can reach significant values. The quality of joint, its strength, deformation of joined elements, equipment of tools, and so on depend on them. Although the load characteristics of the FSW process appear in many publications, their analysis is limited. Most often they come down to determine the maximum axial force recorded during the process, without analyzing its variability.

## 2. Experimental Work

The experimental research included FSW butt joints of magnesium AZ31 and aluminum 2024 T3 alloys. The experiments were carried out on a specially adopted CNC milling machine MAKINO PS95. A cylindrical tool made from tungsten carbide was used (Figure 1). Tool dimensions were adjusted to a material sheet thickness according to algorithm shown in the literature [9]. Generally, it was assumed that the ratio of shoulder diameter to pin diameter should be about 4. Both the pin and the shoulder of the tool had smooth cylindrical shape. The tool worked without any tilt angle; it was set in perpendicular direction to the surface of welded materials. All sheet materials used in experiments were 1 mm in thickness. The blank sheet dimensions were 180 mm × 100mm. A backing plate (table) with two holders constituted the fixture to firmly hold two pieces of joined sheets.

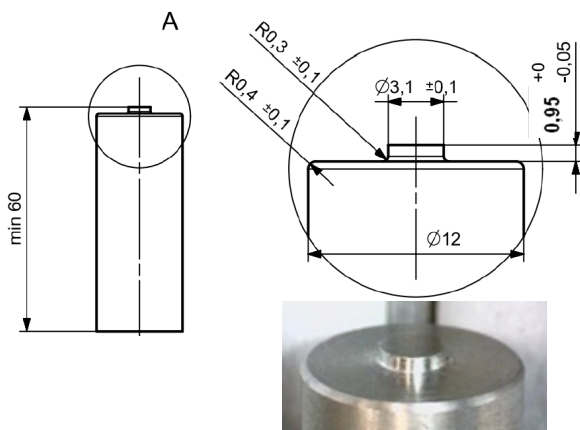


**Figure 1.** Shape and geometry of the tool used in the tests.

The axial (Z axis) and lateral (X and Y axes) forces reacting during FSW process were measured using high-sensitive

piezoelectric dynamometer developed by Kistler. Fixing table with sheet pieces was installed on a machine working plate by the Kistler dynamometer (Figure 2).

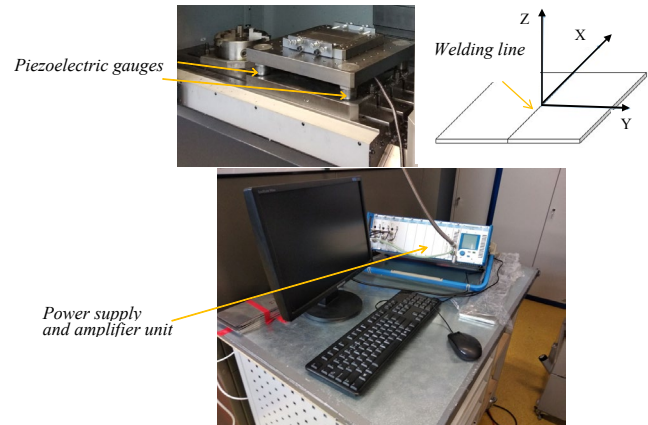


**Figure 2.** Force measurement system.

It consisted of four piezoelectric force sensors calibrated in range from 0 to 60 kN. All sensors were connected via adder to a charge amplifier. The force data could be acquired with a maximum sample rate per channel of 200 kHz and 16-bit resolution. The actual sample rate used during the data recording was 1 kHz. The X axis was oriented along welding line (butt joint line) and the Y axis was perpendicular to that line.

Only 175 mm long butt joints were made. Setup of the tool shoulder, in vertical direction, was chosen as 0.0 mm according to the sheet pieces upper surface. FSW welding experiments were carried out with constant values of rotational speed and welding speed, which were equal to 2,000 rpm of rotation speed and 280 mm/min of travel speed for magnesium alloy AZ31 and 2,000 rpm of rotation speed and 50 mm/min of travel speed for aluminum alloy 2024, respectively. The dwelling time was same for all joints and it was 10 s. Tool plunging in and out stages were realized with tool feed rate of 5 mm/min. Visual evaluation of the joints showed that they were done properly, they have no visible defects, and the face and root surfaces were smooth and uniform. A small flash on the surface of the weld face was allowed.

## 3. Analysis of Force Diagrams

There are three stages in FSW process: plunging, dwelling, and welding, as it was pointed by Assidi et al.[10]. In the first stage plunging, the tool pin is sunk into the sheets to be welded, until the tool shoulder gets a contact with joined sheets surface. In the second stage dwelling, the pin keeps the assumed immersion depth and rotating movement without

any linear translation, so heat conditions of welding process are stabilized. During the third stage welding, the rotating tool moves along the joint line and welds the materials.

Welding forces diagram obtained for magnesium AZ31 alloy is shown in Figure 3. The diagram is divided into three stages as it was mentioned earlier. Each stage has particular duration, which, for the plunging and welding stages, was the result of the tool feed rate and, for the dwelling stage, was established based on preliminary researches.

As it can be observed, the Z-axis force ( $F_z$ ) plays an important role in FSW process; this value is almost 20-fold greater than the force values recorded in the X ( $F_x$ ) and the Y ( $F_y$ ) axes directions. The greatest  $F_z$  force is obtained at the end of the plunging stage and it is diminished at the dwelling stage. In the beginning of the welding stage, when a feed motion of the tool is released, all forces diminish for a short time and then grow and stabilize on a specific force level. During plunging and dwelling stages,  $F_x$  and  $F_y$  forces have almost the same values and variability. They differ at the beginning of the welding stage but the same variability is maintained; smaller force values are recorded in X direction, that is, in the welding line direction.

The analysis of FSW forming forces variability requires an analysis of joined material properties and welding process conditions. Solidus temperature of AZ31 alloy is about 605°C (as shown in Mg-Al phase equilibrium diagram in [11]), so the FSW process temperature can be estimated at ~430°C (it is about 0.8 of material melting temperature).

The main alloying element is aluminum, and in low temperature magnesium with aluminum forms a solid solution  $\alpha$  (hexagonal lattice structure) and intermetallic phase  $Mg_{17}Al_{12}$ , so magnesium alloys are very brittle at room

temperature (only one slip plane (0001)). In temperature above 200°C, the other slip planes are activated that facilitates plastic deformation. As it is shown in [12], the temperature range between brittle and ductile behavior of magnesium alloy MgAl6Zn is very narrow and is only 12°C (from 208°C to 220°C). Achieving the temperature of 200°C is also associated with the recrystallization phenomenon of AZ31 alloy [13].

The FSW process always starts with the tool plunging action into joined materials. The forces recorded in this welding stage are shown in Figure 4. The increase in forces from zero value occurs when the face of the tool pin reaches the surface of joined materials. The thrust force  $F_z$  increases and reaches the maximum value (~3.5 kN) at approximately 4 s. This time is needed to frictional heating of the materials to temperature of about 200°C, exceeding which causes AZ31 alloy to become ductile. The unit pressure exerted by the tool pin face on joined materials surface is in this maximal point of ~464 MPa. At this stage of the process, unit pressures reach the highest values which have an impact on a quick tool wear. In the work of Mishra and Ma [1], it is proposed to preheat the initial plunge region of materials before plunging the pin to reduce the tool wear. During further penetration of the tool pin into sheet pieces, the temperature increases and the yield stress of materials decreases which reduces the unit pressure on the face surface of the pin to value ~358 MPa in the local minimum. During this period, the material is extruded by pin and it flows on its periphery in the upward direction.

When fluctuations of forces in the graphs occur, the extruded material is entering into contact with the tool shoulder. The next local minimum of  $F_z$  force is the result of balancing the phenomenon of heating the material and filling the space under the tool shoulder. The unit pressure 20 MPa was

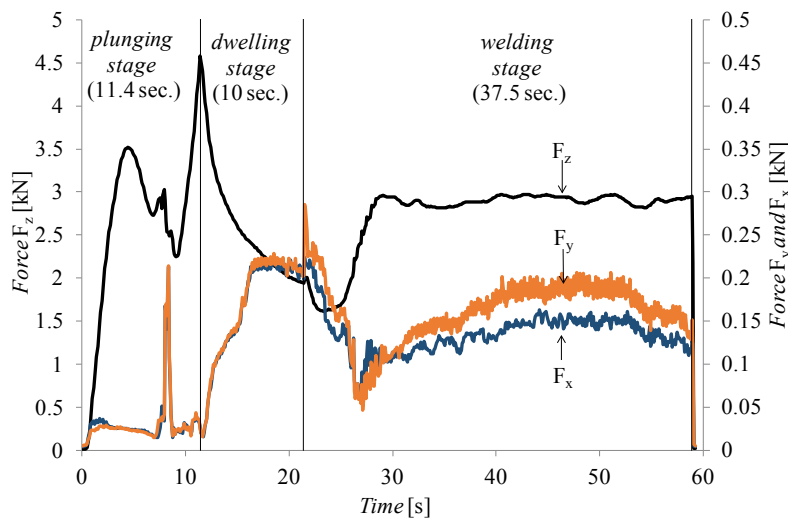
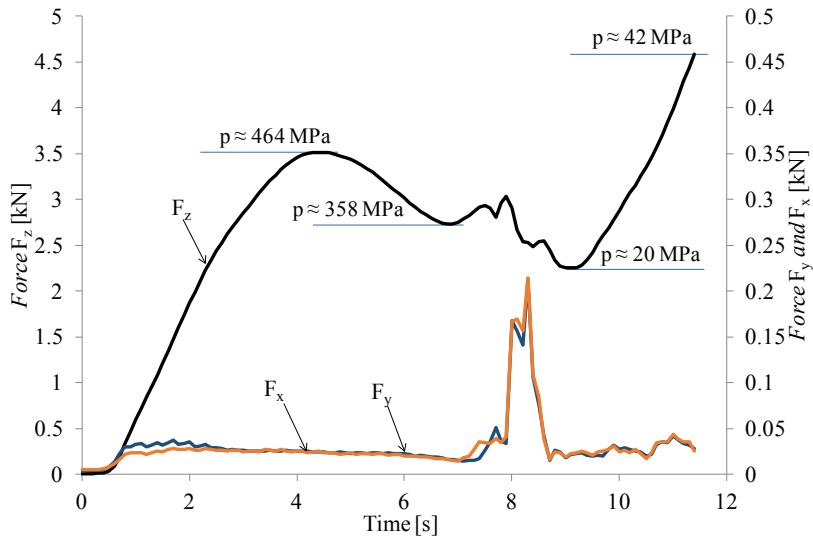


Figure 3. Welding force diagrams recorded for magnesium alloy AZ31 (rotation speed 2,000 rpm and travel speed 280 mm/min).

calculated assuming that the tool thrust force  $F_z$  is evenly distributed over the face surface of the pin and the shoulder (this assumption results from the inability to measure the forces carried separately by the pin and shoulder). Further plunging movement of the tool increases  $F_z$  force as the pressure of the material under the pin and shoulder increases. The increase of  $F_z$  force takes place until the plunging movement of the tool stops. At the end of plunging, on the shoulder periphery the material flows outward and upward due to the extrusion caused by the shoulder plunge motion. This extruded material creates a small flash on the face surface of the weld. The average unit pressure exerted by the tool at the end of the

plunging stage is 42 MPa.

The dwelling stage starts from maximal  $F_z$  value obtained at the end of plunging (Figure 5). During this stage, only the tool rotates without any translation movement. While the tool rotates, frictional and plastic deformation heating causes the rise of temperature and the reduction of material flow stress. The range of the heated and plasticized zone expands. This causes a sharp decrease of forming force  $F_z$  and increase of lateral forces  $F_x$  and  $F_y$  is observed (a duration of about 5 s later). At a later stage, the process thermal conditions stabilize and the process proceeds with a slight gradual decrease in the value of forces. Based on the above, it can be concluded



**Figure 4.** Force diagrams recorded at the plunging stage (magnesium alloy AZ31: rotation speed 2,000 rpm and travel vertical speed 5 mm/min).

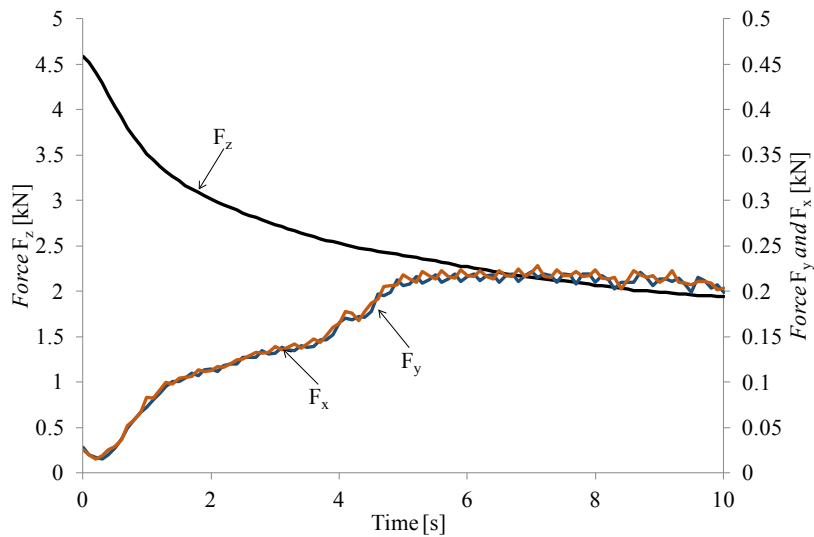


**Figure 5.** Force diagrams recorded at the dwelling stage (magnesium alloy AZ31: rotation speed 2,000 rpm).

that the time of this stage could be limited to about 5 s (it is not 10 s as it was assumed) after which the process passes to the welding stage.

The welding stage begins after starting a linear feed of the welding tool. The linear motion of the tool causes a temporary drop in the formation of force  $F_z$  (Figure 6).

This decrease in force can be explained by the release of material closed and compressed under the face surfaces of the shoulder and the pin and drop of the material pressure. In the further phase of the welding stage, the force  $F_z$  increases to a new stabilized level which is the result of a new (moving along the tool) temperature field. As a result, the welding stage can be divided into two substages: unstable and stable welding. The average unit pressure exerted by the tool is

about 26 MPa. As mentioned earlier, the values of the forces  $F_x$  and  $F_y$  differ at this stage.

When welding aluminum 2024 sheets, the same process parameters as for the magnesium AZ31 alloy were retained, except for the welding speed which was different. Good quality joints were obtained at the significantly lower welding speed of 50 mm/min. A similar character of welding force graphs was obtained (Figure 7), however, the duration of the welding stage is much higher (210 s) because the same length (175 mm) of the welding stage was kept.

Thermal and mechanical properties of aluminum 2024 alloy differ from magnesium AZ31 alloy and that is the reason for differences in forces and unit pressures values. The specific heat of aluminum alloy is less than that of magnesium alloy

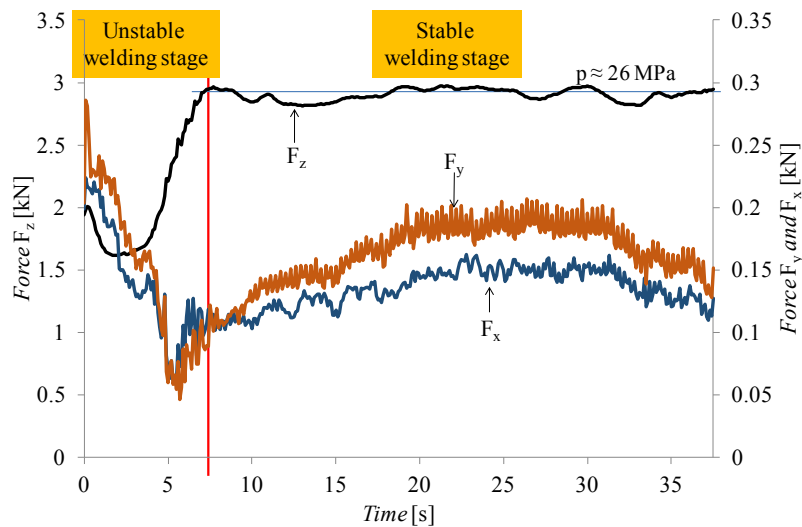


**Figure 6.** Force diagrams recorded at the welding stage (magnesium alloy AZ31: rotation speed 2,000 rpm and travel speed 280 mm/min).

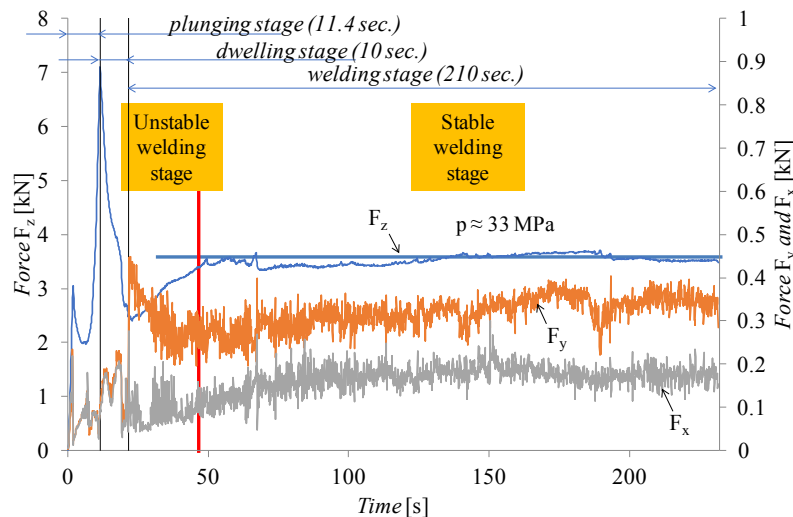


**Figure 7.** Welding forces diagram recorded for aluminum alloy 2024 T3 (rotation speed 2,000 rpm and travel speed 50 mm/min).

(by approximately 150 J/(kg×K) [13]), which means that less heat is needed to increase the temperature locally by the same amount. This is very important in the initial phase of the FSW process, when the temperature gradient in the materials to be joined around the rotating tool is determined. Therefore, in the case of aluminum alloy, at the plunging stage, the lower force  $F_z$  (~3 kN) exerted by the tool pin face at the first maximum point was recorded; the duration to reach this point was also shorter (about 2 s). Thermal conductivity and thermal expansion coefficients are comparable for these materials [13]. The FSW process temperature of aluminum 2024 alloy, calculated as 0.8 solidus temperature ( $T_s \gg 570^\circ\text{C}$  [13]), is about  $401^\circ\text{C}$ . This temperature value is about  $30^\circ\text{C}$  lower than the value estimated for FSW process of magnesium AZ31 alloy. Lower temperature value can explain higher force  $F_z$  and higher mean unit pressure (63 MPa) at the end of the plunging stage and at the welding stage (33 MPa) than the one recorded for magnesium alloy. This is also confirmed by the literature data contained in the source [13], where for these two alloys at the same elevated temperature of  $371^\circ\text{C}$  the yield strength values are 14 MPa for magnesium alloy and 28 MPa for aluminum alloy, respectively. This may justify the differences in the values of registered forces in the FSW welding process of these materials, that is, welding forces of aluminum alloy are higher than magnesium alloy.

#### 4. Conclusions

Forming force diagrams are a very extensive and important source of knowledge about the FSW welding process. Their variability during the welding process reflects all changes in mechanical properties of joined materials due to temperature changes generated during the process. They also reflect the type of movement of the forming tool at individual stages of the process (vertical plunge motion, rotary motion in the immersion, and welding linear feed). Knowledge of forces allows to estimate the amount of unit pressure at subsequent stages of the welding process, as well as to predict tool life and wear. When analyzing recorded diagrams, many general conclusions could be formulated, and most important of them are presented as follows:

- The forming forces of FSW joint depend strongly on the individual properties and microstructure of materials to be joined and on a variability of these properties in a wide range of temperatures, from ambient temperatures to temperatures close to the melting point.
- The highest unit pressure exerted by the FSW tool occurs at the beginning of the plunging stage, and the greatest welding force occurs at the end of the plunging stage and in the beginning of the dwelling stage.
- The largest force acts in the direction of the Z axis (the axis of forming tool) and it plays an important role in the FSW process; its value is almost 20-fold greater than the forces recorded in the X and Y axes directions. This force ( $F_z$ ) is generally identified as the welding force.
- Comparing the welding forces of two alloys from the group of lightweight materials used in aviation, that is, aluminum alloy 2024 and magnesium alloy AZ31, higher values were obtained in the case of the aluminum alloy 2024.

#### References

- [1] R.S. MISHRA, Z.Y. MA: Friction stir welding and processing. *Mater. Sci. Eng.*, **50**(2005), 1-78.
- [2] P. HEURTIER, et al.: Mechanical and thermal modelling of friction stir welding. *J. Mater. Process. Tech.*, **171**(2006), 348-357.
- [3] O. LORRAIN, et al.: Understanding the material flow path of friction stir welding process using unthreaded tools. *J. Mater. Process. Tech.* **210**(2010), 603-609.
- [4] D.H. CHOI, S.K. KIM, S.B. JUNG: The microstructures and mechanical properties of friction stir welded AZ31 with CaO Mg alloys. *J. Alloy. Compd.*, **554**(2013), 162-168.
- [5] G.G. ROY, R. NANDAN, T. DEBROY: Dimensionless correlation to estimate peak temperature during friction stir welding. *Sci. Technol. Weld. Joining.*, **11**(2006)5, 606-608.
- [6] S. MALARVIZHI, V. BALASUBRAMANIAN: Influences of tool shoulder diameter to plate thickness ratio (D/T) on stir zone formation and tensile properties of friction stir welded dissimilar joints of AA6061 aluminum–AZ31B magnesium alloys. *Mater. Des.*, **40**(2012), 453-460.
- [7] T. BALAWENDER, Ł. MICAŁ: Influence of friction stir welding tool geometry on tensile strength of the joint. *ZN PRZ. Mechanika*, **88**(2016), 299-306.
- [8] P. MYŚLIWIEC, R.E. ŚLIWA, R. OSTROWSKI: Possibility of joining thin sheets of Al, Mg alloys and Ti GRADE 3 in FSW process. *Met. Form.*, **XXVIII**(2017)4, 263-280.
- [9] Y.N. ZHANG, et al.: Review of tools for friction stir welding and processing. *Can. Metall. Q.*, **51**(2012)3, 250-261.
- [10] M. ASSIDI, et al.: Friction model for friction stir welding process simulation: calibrations from welding experiments. *Int. J. Mach. Tools Manuf.*, **50**(2010), 143-155.
- [11] J.L. MURRAY: The Al-Mg (aluminum-magnesium) system. *Bull. Alloy Phase Diagrams*, **3**(1982)1, 60-74.
- [12] Extrusion. Second Edition, ASM International, Materials Park, Ohio, USA, 2006. Available online: [www.asminternational.org](http://www.asminternational.org).
- [13] Properties and Selection: Nonferrous Alloys and Special-Purpose Materials, ASM International Handbook, Vol. 2, USA, 1992